Christopher Doerfelt, Thomas Feldmann, Renaud Daenzer, and George P. Demopoulos

Stability of Continually Produced Fe(II)/Fe(III)/As(V) Co-Precipitates under Periodic Exposure to Reducing Agents

Published in:
Chemosphere 138 (2015), pp. 239-246

doi: 10.1016/j.chemosphere.2015.05.096
http://www.sciencedirect.com/science/article/pii/S0045653515005834

Stability of Continuously Produced Fe(II)/Fe(III)/As(V) Co-Precipitates under Periodic Exposure to Reducing Agents#

Christoph Doerfelt[a], Thomas Feldmann[a], Renaud Daenzer[a] and George P. Demopoulos[a,*]
[a]Department of Mining and Materials Engineering, McGill University, 3610 University Street, Montreal, QC, Canada, H3A 0C5

*Corresponding author
Email address: george.demopoulos@mcgill.ca (George P. Demopoulos), Phone: +15143982046
Published in: C. Doerfelt et al. / **Chemosphere** 138 (2015) 239–246 (June 15, 2015)

Abstract

Arsenic mobilized during ore processing necessitates its effective removal from process effluents and disposal in environmentally stable tailings. The most common method to accomplish this involves co-precipitation with excess ferric iron during lime neutralization. The precipitates produced are stable under oxic conditions. This may not be true, however, under sub-oxic or anoxic conditions. In this context, the potential stabilizing role of ferrous iron on arsenic removal/retention becomes important. As such, this work investigates the removal and redox stability of arsenic with ferrous, ferric and mixtures of both. The stability of produced solids is monitored in terms of arsenic release over time. It was found that ferrous was very effective for arsenic (V) removal with Fe(II)/As(V)=4, reducing its concentration down to <15 ppb via the apparent formation of ferrous arsenate. The presence of Fe(II) seemed to favor an oxidation path towards goethite (and possibly scorodite) formation in the aged bench-scale tailings. When pH and E_h were regularly adjusted with lime and sulfite or sulfide, slightly higher arsenic amounts were released (1-5 mg L^{-1}); ferrous again was found to oxidize. Hence, it is concluded that Fe(II)/Fe(III)/ As(V) co-precipitates are quite robust against incidental reducing agent exposure.

Keywords: ferrous arsenate, continuous co-precipitation, effluent treatment, stability, reducing agent

1 Introduction

Management of voluminous waste tailings generated by the mining and metallurgical industries requires that pollutants are stable over the long term for the protection of the environment. While solidification/stabilization technologies can in principle be used (Shih and Lin, 2003; Singh and Pant, 2006) they are not considered economically feasible in the case of voluminous wastes. Instead the co-precipitation of arsenic(V) with ferric by lime neutralization is a widely used method for arsenic removal from acidic sulfate containing effluents (Harris, 2003; Langmuir et al., 1999). According to the US EPA, it is the “Best Demonstrated Achievable Technology (BDAT)” (MSE Technology Applications Inc., 1998). Laboratory scale research has shown that a molar ratio of Fe(III)/As(V)$\geq$3 is needed for complete arsenic removal (Harris and Monette, 1988; Krause and Ettel, 1989). Arsenic is preferably in its pentavalent state due to lesser mobility (Dzombak and Morel, 1990; Korte and Fernando, 1991) and lesser toxicity than As(III) (Styblo et al., 2000).

Until recently, it was believed that arsenic was stabilized only through adsorption onto ferrihydrite ($FeOOH \cdot 12H_2O$) (Robins et al., 1988). Experimental results from low concentration solutions supported these considerations (Waychunas et al., 1993). Chen et al. found that co-precipitation from relatively high arsenic concentration solutions can lead to a stoichiometric ferric arsenate ($FeAsO_4 \cdot xH2O$, co-precipitated along ferrihydrite) phase depending on final neutralizing pH (Chen et al., 2009). Other experimental studies support these findings (Langmuir et al., 2006; Le Berre et al., 2007). Ferric arsenate was also shown to form on the surface of ferrihydrite following adsorption at lower pH (Jia et al., 2006).

The discharged tailings are very complex mixtures of elements so many of potentially beneficial (like Ca, Ni or Al (De Klerk et al., 2015, 2012; Harris, 2000; Jia et al., 2005)) or deleterious (like silica (Swedlund and Webster, 1999)) species already present can impact on the stability of the tailings and their role has to be investigated (Swedlund and Webster, 1999). Not much is known about the effect of ferrous, although widely present in acidic leaching effluents and tailings (Daenzer et al., 2014; Langmuir et al., 1999; Mahoney et al., 2007).

As shown by the work of McCreadie, reducing conditions can develop in the tailings management facilities (McCreadie et al., 2000). These are threatening regarding arsenic remediation as ferric containing solids can undergo reductive dissolution reactions leading to arsenic release. The possible threat originating from anaerobic, strongly reducing conditions to stability of arsenic waste has been stated by Al-Abed et al. (2007), who only studied the influence of redox potential under oxidizing and mildly reducing conditions. In this context, co-precipitating ions like ferrous, as it is already reduced, are interesting to be looked at, because Fe(II)-As(V) interactions can potentially stabilize arsenic in reducing environments. There have been some previous studies on Fe(II)-Fe(III)-As(V) systems. Mukiibi et al. (2008) investigated the effect of pre-adsorbing Fe(II) onto ferrihydrite with subsequent arsenate adsorption. It was found that Fe(II) increased sorption capacity of ferrihydrite. Similar results were obtained by Roberts et al. (2004). Therefore, the scope of this work is to investigate the release of arsenic from ferrous-containing Fe(II)/Fe(III)/As(V) co-precipitates, produced in a two-stage continuous circuit by lime neutralization (Jia and Demopoulos, 2008), when exposed to doses of different reducing agents such as SO_3^{2-} and S^{2-}.

2 Materials and Methods

2.1 Co-precipitation Circuit and Procedures

For the production of solids, a bench-scale 2-reactor (1.6L each) continuous co-precipitation (CCPTN) circuit was used, as described elsewhere (De Klerk et al., 2012). A feed solution with varying Fe(II)/Fe(III)/As(V) molar ratios (Fe(tot)/As(V)=4) was fed at fixed flow rate to give 1 hour mean retention time per reactor. Tests were run in duplicate. The pH was kept constant at pH=4 (Tests CD3 and 4) or 6 (CD2) in reactor 1, and 8 in reactor 2, using 2 mol L^{-1} $Ca(OH)_2$ slurry. After the circuit reached steady-state (De Klerk et al., 2012) slurry was collected for long-term stability tests. pH and E_h values were logged on a computer.

2.2 Stability Testing Procedure

Solids produced in the co-precipitation experiments were exposed to stability testing under various pH and E_h conditions. After the steady-state solids were collected in the form of a slurry, they were allowed to settle in a 4 L graduated cylinder. Half of the aqueous phase was decanted to double the solid/liquid ratio. Then the slurry was homogenized and filled into four 500 mL wide-mouth Nalgene bottles. Every co-precipitation experiment therefore generated four samples, which initially were equivalent and then treated differently during stability testing by either adjusting or not pH (“Drift” and “Oxic” samples) and E_h (“Sulfite” and “Sulfide” samples).

2.2.1 Sampling

The slurries were agitated with magnetic stirring for a total of 7.5 minutes. During this time frame the slurries were, depending on the sample type, sampled only (“Drift” samples), pH adjusted (“Oxic”) and sampled or pH and E_h adjusted and sampled (“Sulfite” and “Sulfide” samples with a target E_h of 250 mV or 0 mV by using 0.1 mol L^{-1} solutions of SO_3^{2-} and S^{2-}, respectively). pH adjustment to pH=8 was done with 1 mol L^{-1} slaked lime for all pH adjusted samples.

2.2.2 pH/Eh adjustment

The slurries were sampled before and after adjustment giving rise to two data points for all samples with the exception of the “Drift” sample, which was not subject to chemical exposure after production. This body of work will focus on the “after-adjustment” samples to evaluate immediate effects of the added chemicals.

2.3 Analysis and Characterization

Fe(II) concentration was determined by a modified dichromate titration method. Total arsenic and iron were analyzed in a Thermo ICAP-6500 axial/radial inductively coupled plasma optical emission spectrometer. Before conducting characterization of the solids, the final aged solids were washed with water to remove gypsum and avoid thus its interference with co-precipitated product identification (dominant XRD gypsum pattern). After washing, the solids were dried for two days at 40°C. XRD patterns for aged solids were recorded on a Bruker DiscoverD8-2D area detector and Co-Kα radiation.

3 Results and Discussion

3.1 Co-Precipitation Performance

The feed composition of the various continuous co-precipitation experiments is given in Table SI-1 (in Supporting Information). The target As(V) concentration in all feed solutions was 1.4 g L^{-1} and the molar ratio of [Fe(II,III)]/[As(V)]=4. Fe(III)/As(V)=4 is used as reference because it is the standard molar ratio in most industrial co-precipitation processes (Jia and Demopoulos, 2008). There were some deviations for the initial concentrations and the molar ratios from the targeted values but overall the experiments are very close to the targeted values and show good reproducibility.

Figure 1 shows an example of iron (in this case ferrous) and arsenic concentration profiles during a co-precipitation test (here: CD2, Fe(II)/As(V)=4). As it can be seen in Figure 1 the circuit has reached steady-state (indicated by the near-plateaus) after 5 h of operation[1]. For the subsequent stability testing work only solids generated after steady-state (after 6.5 h) was reached were used. The initial Fe(II) concentration was 4,021 mg L^{-1}. Roughly 10% loss of ferrous per reactor can be attributed to oxidation due to air intake by the agitated reactors. The dashed lines represent ferrous concentrations in the filtrate. The difference of $Fe_{(tot)}$ and $Fe(II)_{filtrate}$ is the amount of ferrous that precipitated. Almost 90% of the ferrous precipitated. The dotted lines represent arsenic concentrations. Less than 0.5 mg L^{-1} As was left in solution at the end of the experiment (R2 filtrate). These plots are useful to evaluate not only that steady-state has been reached but also the co-precipitation of As(V) with iron (in this case Fe(II); similar evaluations can be done for the other co-precipitation tests (Table SI-2 in Supporting Information)).

[1] It is clarified that the anomalous spike in As concentration seen at time=2 hours is due to apparent experimental error that occurred during sampling. This can be verified with the duplicate test results reported in Figure S1.

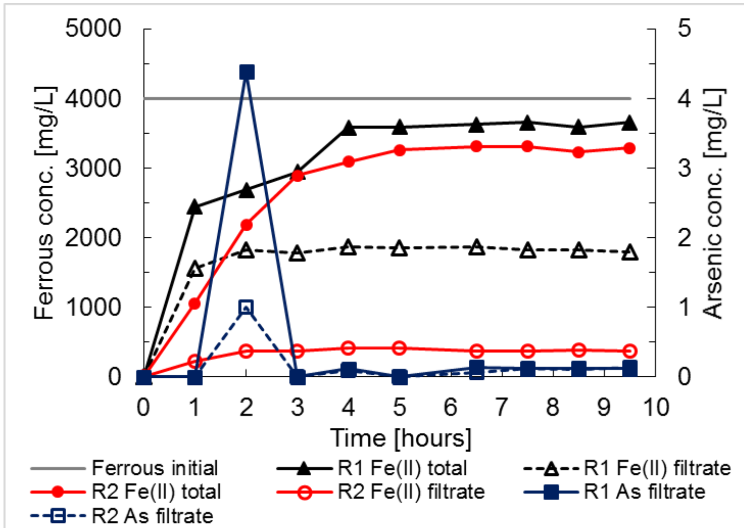

Figure 1 CD2 (Fe(II)/As(V)=4): Ferrous and arsenic concentration profiles during co-precipitation

First of all the amount of ferrous and arsenate precipitated in reactor 1 should be noted (Figure 1 and Table SI-2). As a reminder, the pH in reactor 1 was 6. As it can be seen ca. 50% of ferrous precipitated in reactor 1 alongside all arsenate. The Fe(II)/As(V) molar ratios that precipitate in reactor 1 were 1.70 and 2.08 for CD2 and CD2b respectively. By comparison in the case of experiment CD1, where only Fe(II) was used, barely any ferrous precipitated without As(V) present, namely 304 mg L^{-1} of ferrous equaling 8.05% of total Fe(II). When this percentage is removed from the ferrous precipitating in CD2 and CD2b, corrected molar ratios of 1.42 and 1.65 are obtained. This is an indirect indication of precipitation of arsenic as ferrous arsenate corresponding to the formula of symplesite ($Fe_3(AsO_4)_2 \cdot 8H_2O$, Fe(II)/As(V)=1.5).

The arsenate removal for Fe(II)/As(V)=4 was as effective as for Fe(III)/As(V)=4 (see experiments CD4/CD4b in Table 1) with 0.121 mg L^{-1} of As(V) remaining in solution. When 50% of the ferric is substituted by ferrous (CD3, CD3b) less than 0.1 mg L^{-1} of arsenate was found in reactor 1, on par with the levels of CD2/CD2b and CD4/CD4b. However in reactor 2 the arsenate values of 1.3 mg L^{-1} and 1 mg L^{-1} were surprisingly relatively high. Previous work with the same experimental conditions only found 0.1 mg L^{-1} As in reactor 2, which fits better into the stability range of CD2/CD2b and CD4/CD4b (Daenzer et al., 2014).

The observed somewhat high amounts of arsenate in these experiments (CD3/CD3b) cannot be explained at this point. Since the main scope of this work was the generation of co-precipitates to evaluate their stability under reducing conditions no further investigation was attempted. Of interest are the widely different E_h values in the various tests (Table 4). Thus by focusing on reactor 2 values, it can be seen the higher the Fe(II) concentration the lower the E_h to be: -450 mV (CD1,CD2,CD2b;Fe(II)= 4 g L^{-1}), -150 mV (CD3 and CD3b;Fe(II)= 2 g L^{-1}) and +400 mV (CD4,CD4b;Fe(II)= 0 g L^{-1}, Fe(III)=4 g L^{-1}). Despite the high variation in E_h co-precipitation of arsenate with iron is very effective.

Another issue that needs to be commented on is the pH of the first reactor. As described elsewhere the standard pH profile of the two-stage co-precipitation process is 4 in reactor 1 and 8 in reactor 2 (De Klerk et al., 2012). This was the case for experiments CD4/CD4b and CD3b. However, in the case of ferrous containing feed solutions a higher pH in reactor 1, namely 6, was applied based on the work by Daenzer et al.(2014). In the latter work it was determined that precipitation of ferrous arsenate takes place at pH>5 hence the selection of pH=6 for reactor 1 (Daenzer et al., 2014) that proved indeed very effective (Table 1 and Figure 1). The test with mixed Fe(II)/Fe(III) feed solution (CD3/CD3b) was run with either having pH 4 in reactor 1 (CD3b) or pH 6 (CD3). As it can be seen in Table 1 in either case arsenic removal was essentially complete in reactor 1 (0.1 mg L^{-1} As).

Table 1 Average steady-state values for all CCPTN experiments.

Experiment	Fe/As	Molar ratio	R1 As [mg L^{-1}]	R2 As [mg L^{-1}]	R1 E_h [mV]	R2 E_h [mV]	R1 pH	R2 pH
CD1	Fe(II)	-	-	-	227.7	-430.8	5.76	8.02

CD2	Fe(II)/As(V)	3.8	0.121	0.113	84.5	-478.4	6.11	7.95
CD2b	Fe(II)/As(V)	4.0	*	0.009	45.5	-457.2	6.00	7.87
CD3	Fe(II)/Fe(III)/As(V)	1.6/2.1/1	0.091	0.321	118.6	-140.5	5.91	8.10
CD3b	Fe(II)/Fe(III)/As(V)	2.1/1.9/1	0.095	0.976	420.4	-189.4	3.96	7.78
CD4	Fe(III)/As(V)	3.7	*	*	734.7	393.0	3.73	7.84
CD4b	Fe(III)/As(V)	3.9	0.017	0.013	749.1	401.5	4.02	7.99

*below detection limit, ≤0.009 mg L^{-1}

3.2 Stability Performance

Steady-state co-precipitates were subjected to long-term stability testing by equilibration with water whose pH and Eh conditions were monitored/adjusted on a regular basis. As summarized in Table SI-1 (in Supporting Information). In the first control series labelled “pH-drift” there was no pH or E_h adjustment applied. In the “oxic” series, samples were maintained at pH 8 with regular lime (1 mol L^{-1}) addition without the E_h being adjusted. Finally in the other two series in addition to pH adjustment (pH=8, with lime), sulfite (SO_3^{2-}) and sulfide (S^{2-}) reagents (0.1 mol L^{-1}) were added regularly for the purpose of maintaining E_h at a “sub-oxic” environment (250 mV) and an anoxic environment (0 mV) respectively.

3.2.1 Stability Performance - pH Drift and Oxic Series

The pH and E_h drift as a function of time during stability testing (room temperature ageing) of the various co-precipitates can be seen in Figure 2 (a) and (b). The Fe(II)/As(V)=4 sample was seen to stabilize at pH=7 after roughly 3 months. When ferrous was introduced into the system, the aged samples became more acidic. The drop in pH was proportional to the amount of ferrous present. Thus the Fe(II)/Fe(III)/As(V)=2/2/1 (CD3b) system stabilized at pH=5 while the Fe(II)/As(V)=4 (CD2b) system drifted to a lower pH=3.5.

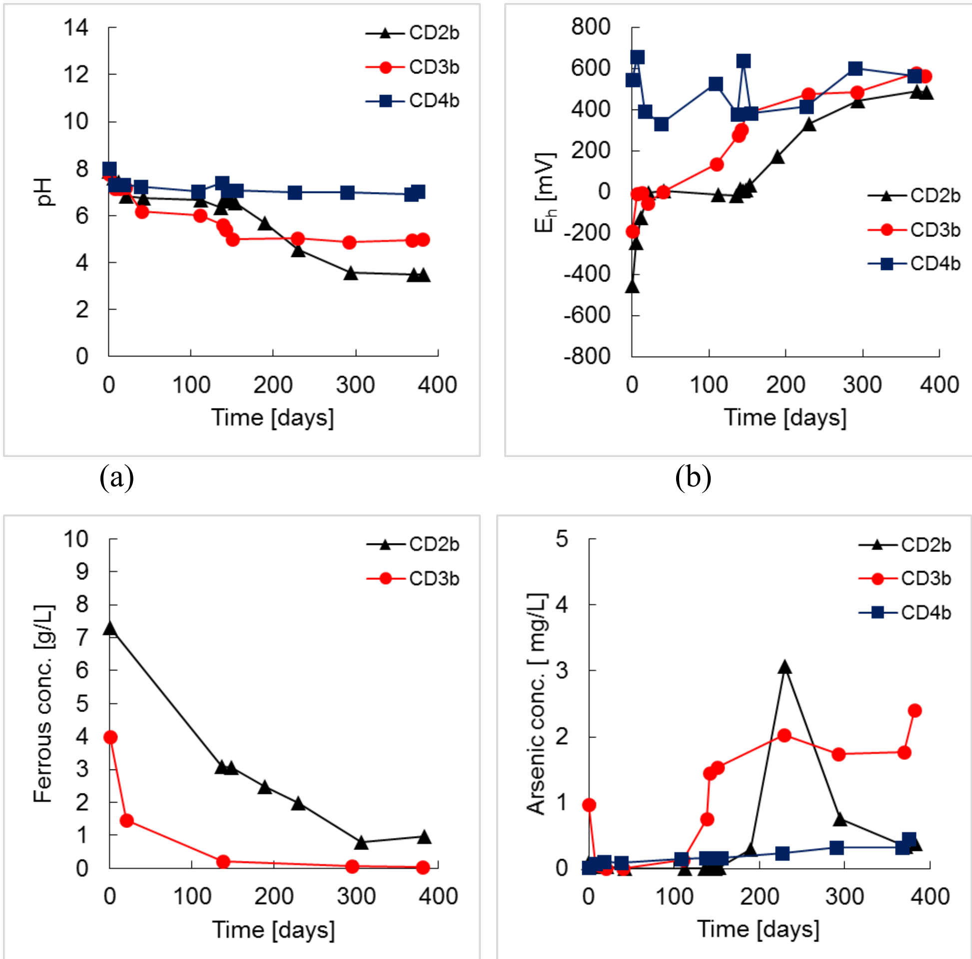

(a) (b)

(c) (d)

Figure 2 pH-”Drift” series: pH evolution (a) and E_h drift (b) as a function of time; ferrous concentrations for CD2b and CD3b during ageing (c) and arsenic concentration (d) for the “Drift” series

At the same time monitoring of the total ferrous concentration (data shown in Figure 2 (c)) revealed its gradual decrease apparently due to oxidation. There was evidence of variable rate of oxidation between soluble ferrous and precipitated ferrous. Thus the CD2b filtrate was found to contain 0.67 g L^{-1} Fe(II) after 383 days, when the total ferrous remaining was only 0.78 g L^{-1}, i.e. only about 15% of the non-oxidized iron being in the solids. This means that overall the solids had only 1.5% of total iron as ferrous left after 383 days. The rest has been oxidized to Fe(III). A similar observation can be made for CD3, where after 381 days only 1% of ferrous was left with all of it being in solution. Both CD2b and CD3b lost approximately 4 g L^{-1} of ferrous in 150 days. There seems to be an initial phase of rapid oxidation of Fe(II). Afterwards the oxidation slowed down, which could be an indication for different Fe(II) phases in the solids, e.g. association of Fe(II) to As(V) and an arsenate-free Fe(II) phase. In the following simplified reaction sequence the oxidation of ferrous arsenate (symplesite) with O_2 will be used as an example to show how solid oxidation can lead to a decrease in pH.

$$2\ Fe_3(AsO_4)_2{\cdot}8\ H_2O + 1.5\ O_2 \rightarrow 2\ Fe(OH)_3 + 4\ AsO_4^{3-} + 4Fe^{3+} + 13\ H_2O \qquad (1)$$

The subsequent hydrolysis of Fe^{3+} releases protons:

$$Fe^{3+} + 3\ H_2O \rightarrow Fe(OH)_3 + 3\ H^+ \qquad (2)$$

The released arsenate re-adsorbs on ferrihydrite (symbolized as $Fe(OH)_3$ for simplicity) or precipitates with ferric to form ferric arsenate (FA) as also indirectly observed in a parallel oxidation study published by our group recently (New ref: Renaud's oxidation paper: Ind. Eng. Chem. Res. 2015, 54, 1738–1747):

$$Fe(OH)_3 + AsO_4^{3-} \rightarrow Fe(OH)_3\text{-}(AsO_4^{3-})_{(ads)} \qquad (3a)$$

$$Fe^{3+} + AsO_4^{3-} \rightarrow FeAsO_4 \qquad (3b)$$

The released arsenic concentration data for the three different drift samples can be found in Figure 2 (d). At termination of the experiments, CD2b (Fe(II)/As(V)=4) and CD4b (Fe(III)/As(V)=4) have a similar arsenic concentration of just below 0.5 mg L^{-1}. However while arsenic release from CD4b gradually increased to reach that point, CD2b exhibits an initial period of approximately 150 days with exceptional arsenic retention. After that point there was a spike in arsenic concentration release, which then lowered to below 0.5 mg L^{-1}. On the other hand, CD3b (Fe(II)/Fe(III)/As(V)=2/2/1) despite the almost 1 mg L^{-1} As reported during co-precipitation in reactor 2 (Table 1) for over 100 days had its arsenic release stabilized below 0.1 mg L^{-1} at the same level as the other two co-precipitates (CD2b and CD4b). After that, arsenic release increased and stayed more or less stable at the 2-2.5 mg L^{-1} level, i.e. a bit higher than the other two co-precipitates.

The origin of the "jump" by CD3b is not clearly understood. After all ferrous is oxidized the sample should behave like CD4b and CD2b at day 385. The spike in arsenic concentration for CD2b after day 189 is interesting, if it is indeed real and not an artifact of a single erroneous sampling point. Arsenic concentration begun to increase after day 149. The same day the total ferrous concentration (slurry digestion) was measured to be 3.05 g L^{-1} with 0.56 g L^{-1} of ferrous in solution. The molar ratio of the resulting 2.49 g L^{-1} Fe(II) in the solids to 2.59 g L^{-1} of As(V) equals 1.29. (The use of g L^{-1} as a unit stems from the direct subtraction of the values mentioned above to avoid altering the results with the incorporation of solid/liquid ratios that were complicated to determine due to ferrous oxidation during drying of the solids.) As established in the co-precipitation section 3.1 this is very close to symplesite (1.5). Hence it is possible that the oxidation of the ferrous arsenate precipitate that formed during co-precipitation led to the initial arsenic release (spike over the period 200-300 days). The subsequent drop can reflect arsenic scavenging by Fe(III) to form ferric arsenate and/or arsenical ferrihydrite (see Equations (1), (2) and (3)). For CD3b, the arsenic concentration increased drastically after all the ferrous was oxidized. Despite certain differences in the final arsenic release levels (especially in the case of CD3b) the generated results suggest that ferrous or mixed ferrous/ferric can essentially stabilize arsenate over the long term the same way as ferric alone, as long as the molar ratio is Fe(II,III)/As(V)C4 and drift oxic conditions prevail.

The oxidation of the ferrous-containing co-precipitates to ferric equivalent compounds was also confirmed by XRD analysis as shown in Figure 3. Reference patterns for ferrihydrite synthesized as described elsewhere (Jia and Demopoulos, 2005) and yukonite synthesized in our laboratory are included (Gomez et al., 2010). Other reference spectra retrieved from the JCPD-cards given, are goethite, 6-line ferrihydrite and scorodite. Distinction between arsenical ferrihydrite and poorly crystalline ferric arsenate is not straight-forward because of their similar two broad peaks (Jia et al., 2005; Le Berre et al., 2007). Comparing CD4b (Fe(III)/As(V)=4) to the reference spectra shows that the aged sample has the main ferrihydrite features. However, the presence of the shoulder at 35° 2-theta along a slight peakshift of the two broad peaks to the left may be taken as evidence of co-existence of poorly crystalline ferric arsenate (Le Berre et al., 2007). The small, sharp peaks in CD4b are background peaks from the aluminum sample holder due to inadequate sample amount.

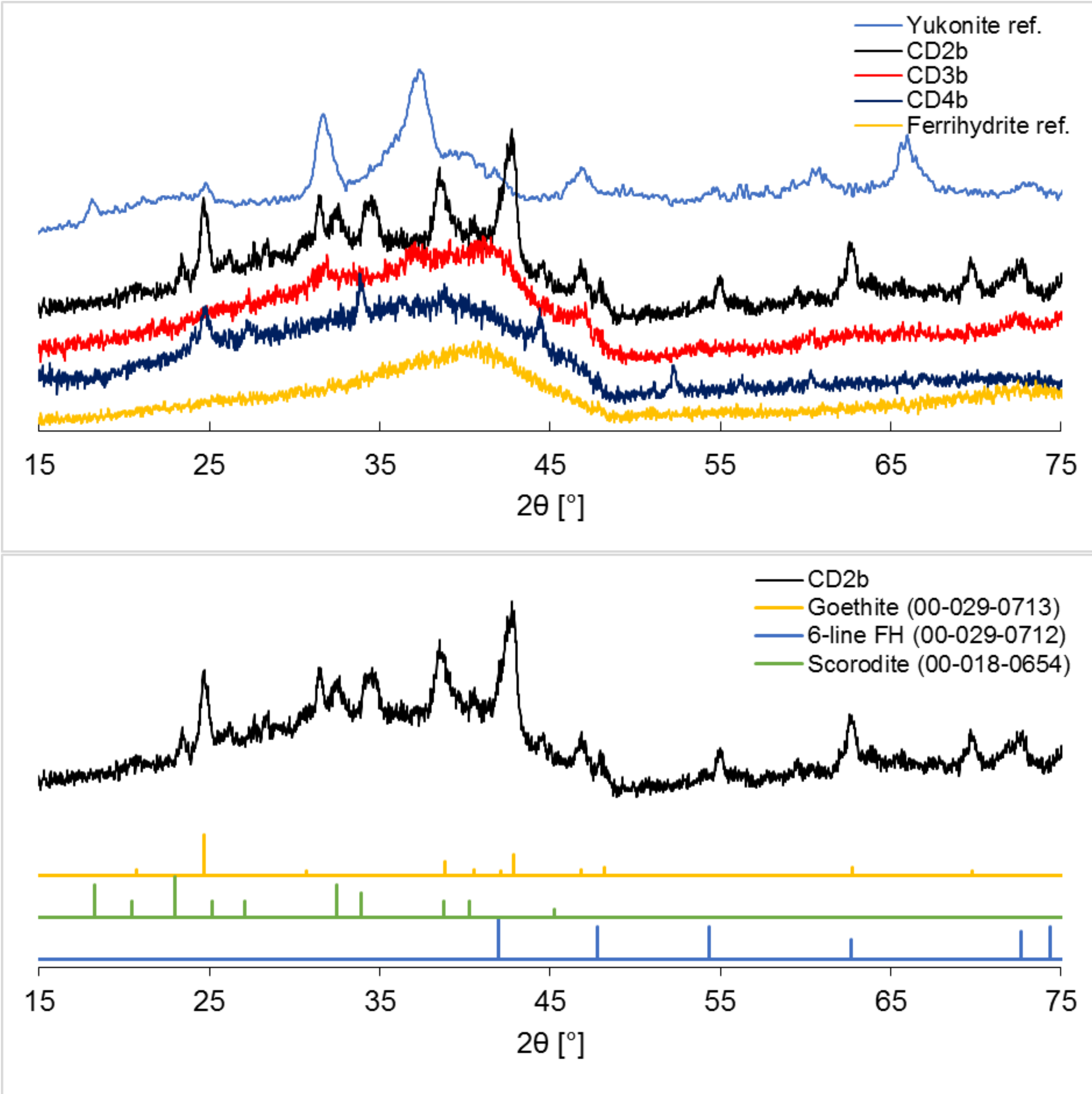

Figure 3 XRD patterns for CD2b/CD3b/CD4b "Drift" series at termination of experiments vs. ferrihydrite (FH) and yukonite reference (top) and CD2b "Drift" series vs. goethite, scorodite and 6- line ferrihydrite (bottom)

CD2b and CD4b feature the two broad peaks as well but this time there are additional small sharp peaks revealing the appearance of crystalline phase features. As such, goethite has been identified to be present possibly resulting from crystallization of ferrihydrite and scorodite crystallizing from ferric arsenate (Le Berre et al., 2008). There seem to be more crystalline phase peaks present the higher the initial ferrous content. Most of these peaks appear to indicate goethite formation as well as 6-line ferrihydrite and for CD2b (pH=3.5) possibly scorodite. The amount of initial Fe(II) seems to be the determining factor as to how much goethite is formed (compare CD2b and CD3b). No yukonite was detected (Jia and Demopoulos, 2008).

The "Oxic" stability series involved adjustment to pH=8 with slaked lime. Samples were taken before and after adjusting the pH. The variation of pH, E_h, arsenic release and iron oxidation as a function of equilibration time are reported in the Supplementary Information part of this paper. The E_h was found to progressively increase reaching relatively stable level at around 400-600 mV over time independent of the initial iron (Fe(II)/Fe(III)) content used as observed also in the "Drift series-see plots in Fig. 2. The rise of E_h was linked to the progressive oxidation of Fe(II) to Fe(III)After 300 days essentially all ferrous was oxidized. The oxidation of the solids was further evidenced by XRD analysis. Similar patterns as with the "pH-drift" series were obtained although in this case the goethite formation signs were less pronounced (see patterns in SI). Table SI-3 summarizes the long-term arsenic release data from this series along the time it took for stable Eh and [As] levels to be reached. The final arsenic release concentrations were about two times higher than the values released in the Drift series. This is attributed to the higher pH of the Oxic series (8 vs. 3.5 (CD2b), 5 (CD3b) and 7 (CD4b)) of the Drift series.

3.2.2 Stability Performance - Effects of Sulfite (SO_3^{2-}) Addition

Additionally to adjusting the pH with slaked lime, in this series the co-precipitates were exposed to frequent sulfite (0.1 mol L^{-1} SO_3^{2-}) addition. Sulfite is a modest reducing agent at pH=8 and this experiment therefore represents a sub-oxic environment, an intermediate between the "Oxic" and "Sulfide" series. In particular in this series the target E_h was 250 mV. The evolution of E_h for the three co-precipitates during stability testing (after adjustment with sulfite addition) is shown in Figure 4 (a). As it can be seen, the E_h increased with time because of the inevitable exposure to air during sampling. Initially up to 150 days for CD3b and 300 days for CD2b the E_h remained below the target 250 mV. The CD4b had an E_h varying between 250 and 350 mV.

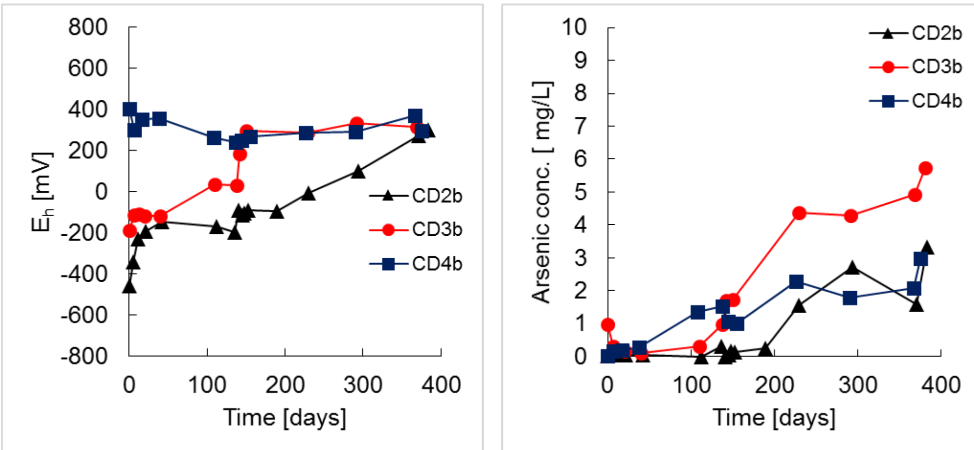

(a) (b)

Figure 4 E_h progression for all "Sulfite" samples (after-adjustment samples) (a) and their arsenic concentration during long-term stability testing (b)

The progression of the released arsenic concentration can be found in Figure 4 (b). Again the trends are the same as for the "Drift" and "Oxic" series, but the final (upper) levels reached are practically the same with the values reached in the Oxic series (same pH=8)- see Table SI-3. In other words, overall no drastic destabilizing effects were introduced by exposing the co-precipitates to periodic sulfite dosing under non-air exclusion conditions. This implies relatively high stability of the produced solids under a sub-oxic environment.

3.2.3 Stability Performance - Effect of Sulfide (S^{2-}) Addition

Sulfide is a strong reducing agent, stronger than sulfite, and in this case the target Eh was 0 mV. The evolution of Eh for the three co-precipitates during stability testing (after adjustment with sulfide addition) is shown in Figure 5 (a). As it can be seen the target E_h of 0 mV was consistently achieved after sulfide addition. However, between adjustments - coinciding with sampling – the E_h tended to increase (as also happened with sulfite) with time due to air infiltration. A good measure of the “up-and-down” E_h variation can be obtained by reviewing the actual data for the CD2b test, shown in Figure 5 (b). Up to ~200 days the Eh did not rise above 100 mV. This was helped by the relatively frequent addition of sulfide but also the presence of large excess of ferrous. Despite this frequent sulfide addition however oxidation of Fe(II) in CD2b (and CD3b) did occur even when the Eh was <100 mV. Thus after 200 days more than 70% of Fe(II) in CD2b has been oxidized (see Figure 6 (a)). The oxidation was essentially complete after 150 days in the case of CD3b and after 300 days in the case of CD2b – note double the time was required for double the ferrous quantity. The full oxidation of the solids was also evident from the XRD patterns that had the same features as found previously for “Oxic” and “Sulfite” solids (patterns shown in the Supporting Information in Figures SI-5 to SI-7).

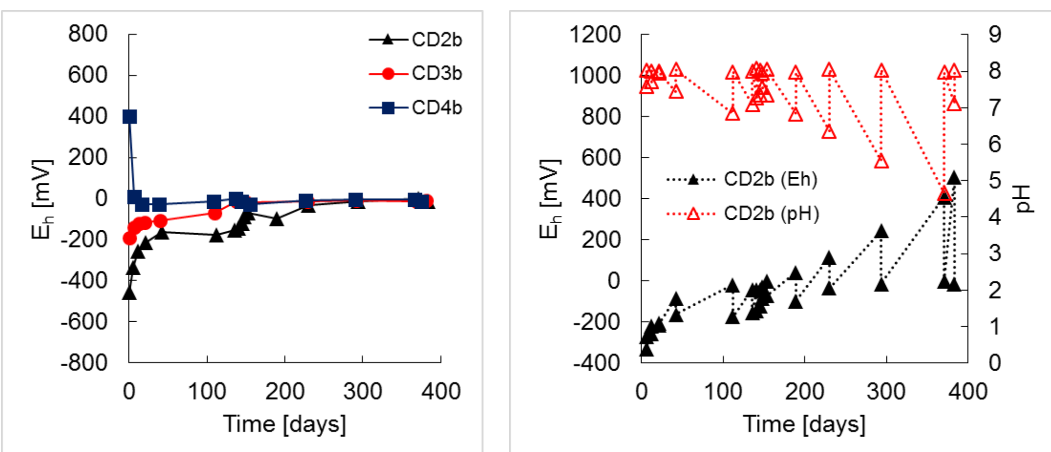

(a) (b)

Figure 5 E_h progression for all “Sulfide” samples after-adjustment samples (a) and E_h-pH progression before and after adjustment for CD2b S^{2-} (b)

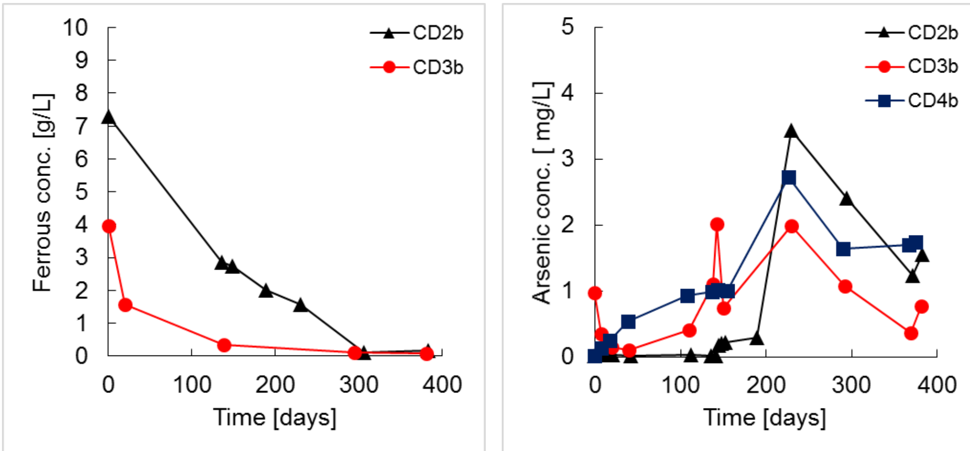

(a) (b)

Figure 6 The oxidation of Fe(II) for all “Sulfide” samples (a) and the arsenic concentrations during stability testing for all “Sulfide” samples (b)

The arsenic concentration released from the different co-precipitates during the S^{2-} stability testing series is presented in Figure 6 (b) (Note that all these data are from samples collected after E_h adjustment to 0 mV). At completion of the stability testing after one year, CD4b (Fe(III)/As(V)=4) had the highest arsenic concentration at 1.74 mg L^{-1}, a concentration that is almost the same with the CD4b “Oxic” sample. Similar values were obtained for CD2b (Fe(II)/As(V)=4). CD3b (Fe(II)/Fe(III)/As(V)=2/2/1) had the lowest arsenate release with about 0.8 mg L^{-1}, which is also a lot lower than the CD3b “Oxic” sample (4.5 mg L^{-1}). Before these low values were attained, all co-precipitates went through a spike in arsenic release, similar with the one observed in the “Drift”, “Oxic” and “Sulfite” series. This is as already discussed most likely linked to oxidation of the ferrous arsenate phase with subsequent arsenate fixation via adsorption on ferrihydrite and ferric-arsenate formation.

Overall the arsenic release data are truly remarkable considering that an aggressive reducing agent like sodium sulfide was used and the E_h potential was kept below 0 mV for at least 200 days-see Figure 5 (b). The “sulfide” samples overall show surprisingly low arsenic release. It is possible that the added S^{2-} actually helped “stabilize” arsenate rather than releasing more for

CD2b and CD3b. Although the sulfide could precipitate arsenic to form As_2S_3 the latter is unstable in oxidizing environments and relatively soluble (Young and Robins, 2000), therefore expected to re-dissolve eventually. Although a number of questions remain, the fact is, that the Fe(II)/Fe(III)/As(V) co-precipitates remained essentially unaffected by exposing them to a strong reducing agent (S^{2-}) in a non air-tight environment.

4 Conclusions

From the data presented in the previous sections the following general trends/conclusions can be drawn:

- Arsenate co-precipitation with ferrous iron is very effective and achieves comparable levels as Fe(III)/As(V) co-precipitation with well above 99.9% arsenate removal.
- The two-reactor continuous co-precipitation tests with Fe(II)/As(V)=4 reveals initial retention of arsenic in the form of ferrous arsenate (symplesite-like) that remains stable until it is oxidized.
- Drift pH leads to more stable precipitates (due to lower attained pH) than adjusted/fixed pH (at pH=8).
- Oxidation of Fe(II)-containing co-precipitates goes through a minor spike in arsenic release before arsenic is stabilized through re-adsorption or ferric arsenate formation. The presence of Fe(II) seems to favor an oxidation path towards goethite (and possibly scorodite) formation in the aged bench-scale tailings.
- Arsenic release is higher (but still) “reasonable” when reducing agents are used, e.g. arsenic release remains below 2 mg L^{-1} at pH near 8 even after one year ageing proving that

Fe(II)/Fe(III)/As(V) co-precipitates are quite robust against intermittent chemical reducing agent exposure like sulfides (-200 mV<Eh<200 mV).

5 Acknowledgements

The work reported here was supported via a NSERC (National Science and Engineering Research Council of Canada) collaborative research grant jointly funded by AREVA Resources Canada and the Cameco Endowment Trust fund (grant number CRDPJ417861-11).

6 References

Al-Abed, S.R., Jegadeesan, G., Purandare, J., Allen, D., 2007. Arsenic release from iron rich mineral processing waste: Influence of pH and redox potential. Chemosphere 66, 775–782. doi:10.1016/j.chemosphere.2006.07.045

Chen, N., Jiang, D.T., Cutler, J., Kotzer, T., Jia, Y.F., Demopoulos, G.P., Rowson, J.W., 2009. Structural characterization of poorly-crystalline scorodite, iron(III)-arsenate co-precipitates and uranium mill neutralized raffinate solids using X-ray absorption fine structure spectroscopy. Geochim. Cosmochim. Acta 73, 3260–3276. doi:10.1016/j.gca.2009.02.019

Daenzer, R., Xu, L., Doerfelt, C., Jia, Y., Demopoulos, G.P., 2014. Precipitation behaviour of As(V) during neutralization of acidic Fe(II)−As(V) solutions in batch and continuous modes. Hydrometallurgy 146, 40–47. doi:10.1016/j.hydromet.2014.03.005

De Klerk, R.J., Feldmann, T., Daenzer, R., Demopoulos, G.P., 2015. Continuous circuit coprecipitation of arsenic(V) with ferric iron by lime neutralization: The effect of circuit staging, co-ions and equilibration pH on long-term arsenic retention. Hydrometallurgy 151, 42–50. doi:10.1016/j.hydromet.2014.11.003

De Klerk, R.J., Jia, Y., Daenzer, R., Gomez, M.A., Demopoulos, G.P., 2012. Continuous circuit coprecipitation of arsenic(V) with ferric iron by lime neutralization: Process parameter effects on arsenic removal and precipitate quality. Hydrometallurgy 111, 65–72. doi:10.1016/j.hydromet.2011.10.004

Dzombak, D.A., Morel, F.M.M., 1990. Surface Complexation Modeling: Hydrous Ferric Oxide, A Wiley-Interscience publication. John Wiley & Sons.

Gomez, M.A., Becze, L., Blyth, R.I.R., Cutler, J.N., Demopoulos, G.P., 2010. Molecular and structural investigation of yukonite (synthetic & natural) and its relation to arseniosiderite. Geochim. Cosmochim. Acta 74, 5835–5851. doi:10.1016/j.gca.2010.07.023

Harris, B., 2003. The removal of arsenic from process solutions: Theory and industrial practice. Hydrometall. 2003 Proc. 1889–1902.

Harris, G.B., 2000. The removal and stabilization of arsenic from aqueous process solutions: past, present and future, in: Young, C.A. (Ed.), Minor Elements 2000: Processing and Environmental Aspects of As, Sb, Se, Te, and Bi. SME, Littleton CO., pp. 3–20.

Harris, G.B., Monette, S., 1988. The Stability of Arsenic Bearing Residues, in: Reddy, R.G., Hendrix, J.L., Queneau, P.B. (Eds.), Arsenic Metallurgy Fundamentals and Applications. TMS (The Minerals, Metals & Materials Society), Warrendale, PA, pp. 469–488.

Jia, Y., Demopoulos, G.P., 2008. Coprecipitation of arsenate with iron(III) in aqueous sulfate media: Effect of time, lime as base and co-ions on arsenic retention. Water Res. 42, 661–668. doi:10.1016/j.watres.2007.08.017

Jia, Y.F., Demopoulos, G.P., 2005. Adsorption of arsenate onto ferrihydrite from aqueous solution: Influence of media (sulfate vs nitrate), added gypsum, and pH alteration. Environ. Sci. Technol. 39, 9523–9527. doi:10.1021/es051432i

Jia, Y.F., Demopoulos, G.P., Chen, N., Cutler, J., 2005. Coprecipitation of As(V) with Fe(III) in sulfate media: Solubility and speciation of arsenic. Arsen. Metall. 137–148.

Jia, Y.F., Xu, L.Y., Fang, Z., Demopoulos, G.P., 2006. Observation of surface precipitation of arsenate on ferrihydrite. Environ. Sci. Technol. 40, 3248–3253. doi:10.1021/es051872+

Korte, N.E., Fernando, Q., 1991. A review of arsenic(III) in groundwater. Crit. Rev. Environ. Control 21, 1–39.

Krause, E., Ettel, V.A., 1989. Solubilities and stabilities of ferric arsenate compounds. Hydrometallurgy 22, 311–337. doi:10.1016/0304-386x(89)90028-5

Langmuir, D., Mahoney, J., MacDonald, A., Rowson, J., 1999. Predicting arsenic concentrations in the porewaters of buried uranium mill tailings. Geochim. Cosmochim. Acta 63, 3379–3394. doi:10.1016/s0016-7037(99)00259-8

Langmuir, D., Mahoney, J., Rowson, J., 2006. Solubility products of amorphous ferric arsenate and crystalline scorodite (FeAsO4·2H2O) and their application to arsenic behavior in buried mine tailings. Geochim. Cosmochim. Acta 70, 2942–2956. doi:10.1016/j.gca.2006.03.006

Le Berre, J.F., Gauvin, R., Demopoulos, G.P., 2007. Characterization of Poorly-Crystalline Ferric Arsenate Precipitated from Equimolar Fe(III)-As(V) Solutions in the pH Range 2 to 8. Metall. Mater. Trans. B 38, 751–762. doi:10.1007/s11663-007-9081-y

Le Berre, J.F., Gauvin, R., Demopoulos, G.P., 2008. A study of the crystallization kinetics of scorodite via the transformation of poorly crystalline ferric arsenate in weakly acidic solution. Colloids Surfaces A Physicochem. Eng. Asp. 315, 117–129. doi:10.1016/j.colsurfa.2007.07.028

Mahoney, J., Slaughter, M., Langmuir, D., Rowson, J., 2007. Control of As and Ni releases from a uranium mill tailings neutralization circuit: Solution chemistry, mineralogy and geochemical modeling of laboratory study results. Appl. Geochemistry 22, 2758–2776. doi:10.1016/j.apgeochem.2007.06-021

McCreadie, H., Blowes, D.W., Ptacek, C.J., Jambor, J.L., 2000. Influence of reduction reactions and solid-phase composition on porewater concentrations of arsenic. Environ. Sci. Technol. 34, 3159–3166.

MSE Technology Applications Inc., 1998. Final report - Arsenic removal demonstration project - Mine waste technology program activity III, Project 9.

Mukiibi, M., Ela, W.P., Saez, A.E., 2008. Effect of ferrous iron on arsenate sorption to amorphous ferric hydroxide. Environ. Challenges Pacific Basin 1140, 335–345. doi:10.1196/annals.1454.024

Roberts, L.C., Hug, S.J., Ruettimann, T., Billah, M., Khan, A.W., Rahman, M.T., 2004. Arsenic removal with iron(II) and iron(III) waters with high silicate and phosphate concentrations. Environ. Sci. Technol. 38, 307–315. doi:10.1021/es0343205

Robins, R.G., Huang, J.C.Y., Nishimura, T., Khoe, G.H., 1988. The adsorption of arsenate ion by ferric hydroxide, in: Reddy, R.G., Hendrix, J.L., Queneau, P.B. (Eds.), Arsenic Metallurgy. TMS (The Minerals, Metals & Materials Society), pp. 99–112.

Shih, C.J., Lin, C.F., 2003. Arsenic contaminated site at an abandoned copper smelter plant: Waste characterization and solidification/stabilization treatment. Chemosphere. doi:10.1016/S0045-6535(03)00519-8

Singh, T.S., Pant, K.K., 2006. Solidification/stabilization of arsenic containing solid wastes using portland cement, fly ash and polymeric materials. J. Hazard. Mater. 131, 29–36.

Styblo, M., Del Razo, L.M., Vega, L., Germolec, D.R., LeCluyse, E.L., Hamilton, G.A., Reed, W., Wang, C., Cullen, W.R., Thomas, D.J., 2000. Comparative toxicity of trivalent and pentavalent inorganic and methylated arsenicals in rat and human cells. Arch. Toxicol. 74, 289–299.

Swedlund, P.J., Webster, J.G., 1999. Adsorption and polymerisation of silicic acid on ferrihydrite, and its effect on arsenic adsorption. Water Res. 33, 3413–3422.

Waychunas, G.A., Rea, B.A., Fuller, C.C., Davis, J.A., 1993. Surface Chemistry of Ferrihydrite 1. EXAFS Studies of the Geometry of Coprecipitated and Adsorbed Arsenate. Geochim. Cosmochim. Acta 57, 2251–2269. doi:10.1016/0016-7037(93)90567-g

Young, C.A., Robins, R.G., 2000. The solubility of As2S3 in relation to the precipitation of arsenic from process solutions, in: Young, C.A. (Ed.), Minor Metals 2000. SME, Littleton CO., pp. 381–391.